

## A Simulation of EOS MISR Data and Geometric Processing for the Prototyping of the MISR Ground Data System

Scott A. Lewicki, Michael M. Smyth, Veljko M. Jovanović, and Earl G. Hansen  
Earth Observations Analysis Systems Section, Mail Stop 169-315,  
Jet Propulsion Laboratory, California Institute of Technology,  
4800 Oak Grove Drive, Pasadena, CA 91109 USA  
T: 818.354.3534 F: 818.393.4802 EMail: scalle@papa.jpl.nasa.gov

### ABSTRACT

This paper describes a modeling system for the simulation of the Multi-angle Imaging Spectro-Radiometer (MISR) instrument push-broom data to be used in the prototyping of the MISR ground data system. The data are being simulated using the known characteristics of the instrument and spacecraft position and pointing. Rendering software obtained from the Digital Image Animation Laboratory (DIAL) at JPL has been modified to model multi-angle push-broom data. Landsat TM data are used as input radiance.

### EXPERIMENT OVERVIEW

#### Instrument Overview

MISR (Diner et al., 1993) will be launched into polar orbit on the Earth Observing System (EOS) AM1 spacecraft in June 1998. It contains nine push-broom cameras to observe at fixed view angles, relative to the surface normal, of 0° (nadir), 26.1°, 45.6°, 60.0°, and 70.5° fore and aft of nadir using charge-coupled device (CCD) line arrays filtered to 443, 555, 670, and 865 nm. The line arrays consist of 1504 photoactive pixels plus 16 light-shielded pixels per array, each 21  $\mu\text{m}$  square. The overlap swath width seen in common by all nine cameras is 360 km, which provides global multi-angle coverage of the entire Earth in 9 days at the equator, and 2 days at the poles. The cross-track instantaneous field of view (IFOV) and sample spacing of each pixel is 275 m for all of the off-nadir cameras, and 250 m for the nadir camera. Along-track IFOV's depend on view angle, ranging from 250 m in the nadir to 825 m at the most oblique angle. Sample spacing in the along-track direction is 275 m in all cameras.

#### Processing Overview

Since the MISR instrument acquires push-broom imagery from nine widely separated locations along the sub-spacecraft track, it takes about seven minutes for any single location along this track to be observed by the nine cameras. The science objectives for the mission require this set of multi-angle images be geolocated to  $\pm 250$  m ( $2\sigma$ ) and co-registered to  $\pm 500$  m along-track and  $\pm 250$  m cross-track ( $2\sigma$ ). These requirements insure accurate placement of MISR data products on a geographical grid, registration with Digital Elevation Models (DEMs) used for topographic corrections, and co-registration of MISR imagery for any particular target acquired on multiple orbits, thereby insuring the ability to separate actual temporal changes on the Earth from misregistration errors.

Achievement of these geometric performance requirements necessitate geometric calibration of the instrument early in the mission to obtain an improved camera model relative to the characterizations obtained pre-flight. The geometric calibration will involve the removal of any static or systematic biases between the true pointing direction and the navigation information supplied from the spacecraft in order to obtain a high-accuracy estimate of the camera pointing. This will be accomplished through correlation of selected MISR imagery with high-resolution, geolocated non-EOS data. After the cameras are geometrically calibrated, the image geolocation and registration requirements stated above will be met by first establishing, early in the mission and for each camera, 233 MISR reference images (one for each orbit in the EOS 16-day repeat cycle) consisting of the most cloud-free views of the Earth observed during those

orbits. The camera geometric calibration information, coupled with a DEM, will enable geolocation of the nadir and off-nadir images using rectification methods. During standard processing, newly acquired images at each angle will be registered with the reference imagery at that angle by a combination of backward projection using image point intersection methods and limited image matching using brightness correlation techniques. The predetermined projection parameters will then be applied in order to generate a complete multi-angle set of ortho-rectified data.

### MISRSIM DEVELOPMENT

In order to prototype all of the elements of the geometric processing described above, data must be acquired which match closely the characteristics of MISR instrument data. Since currently there does not exist a push-broom instrument with the combination of extreme forward and aft views of MISR, the data must be simulated. A technique known as *terrain rendering* is employed to model the topographic effects of imaging the Earth's surface at extreme viewing angles. Terrain rendering is the mapping of image data onto DEMs to produce a three-dimensional simulation of the actual surface.

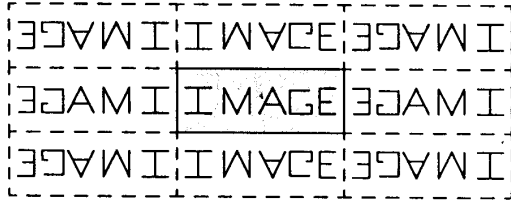
Rendering software was acquired from the Digital Image Animation Laboratory (DIAL) at JPL. The DIAL has used this code very successfully to produce simulated flights over the terrain of California and the planet Venus (Stanfill, 1991). This software uses a ray-casting algorithm, where a given view is calculated from a single point in space (or *eye point*) relative to the location of the terrain. The eye point's field of view and aspect ratio define a view-plane perpendicular to the line of sight representing the image to be computed. For the DIAL software, the view-plane is a finite rectangular plane such as would be seen by a frame camera. For use in MISRSIM, the software was adapted such that the view-plane represented what was seen by a single line-array CCD.

### MISRSIM PROCESS FLOW

#### Data Preparation

To simulate the radiance image data, Landsat Thematic Mapper (TM) scenes were used. A Universal Transverse Mercator (UTM) plate of an area of central Mexico with a map scale of 28.5 m was acquired. This image also was identified as representing an area of high relief and strong image texture. TM Band 3 (red) was separated from the data to model the MISR red channel. A DEM with 100 m postings which had already been registered to the UTM plate was resampled to the Landsat scale. Each UTM plate covers approximately 2° of longitude and 1° of latitude. This is not sufficient to cover the width of a MISR swath. In addition, 1° of latitude corresponds to a simulated orbit segment of no more than 15 seconds. In order to cover the full width and length of a swath segment corresponding to a 7 minute period, where an area is observed by all cameras, the following technique is used: First, the ascending node of the MISR orbit path is chosen such that the ground track passes through the central point of the input region. Then, a Space-Oblique Mercator (SOM) projection associated with this orbit path is defined. The limits imposed by the size of the input are extended by reflecting the original input region in the necessary directions throughout this

SOM map. The smooth transition of the ground surface is provided for by flipping the images and DEM values at the boundaries as shown below:



#### Orbit Simulation

An orbit program was written at JPL to model the expected EOS AM1 orbit. The program works in the following way: First, orbit positions are calculated at 1 minute intervals by directly integrating the force equations, written as a standard multipole expansion, using the initial conditions for the predicted orbit. Effects up to second order are included. This calculation is performed once and stored in a file for further runs of the program. Then, orbit positions are calculated at 40.8 ms MISR sampling intervals by using a cubic spline fit to the 1 minute interval data. Transformations to account for the Earth's rotation are included.

The orbit program generates, for each time interval, the spacecraft position and the intercept of each camera's boresight with the Earth at sea level, which will be the center of the MISR swath. These positions are expressed in map coordinates (latitude, longitude, and altitude above the reference ellipsoid). Once the spacecraft position and swath center (i.e., the beginning and end of a ray cast from a camera to the surface) are read, they are transformed to geocentric cartesian coordinates (GCC). Based on these coordinates, another coordinate system, the local renderer (LR), will be defined, which is used for implementation purposes. It has the following characteristics: The positive z-axis points from the Earth's center to the spacecraft; the positive x-axis passes through the swath center and is perpendicular to the z-axis; and the positive y-axis completes the right-handed coordinate system. The relationship between these coordinate systems is shown in Figure 1.

During its processing the rendering code will need to know if points along a ray are above or below the DEM of the surface within a predefined tolerance. The check is performed in the following manner: The LR coordinates of each point are transformed to GCC and elevation. The GCC is transformed to the SOM projection. Next, the SOM value is propagated through the original image. Finally, the SOM is transformed to UTM allowing the DEM or radiance to be read from the original image.

Using exact formulas for these coordinate transformations would provide the best accuracy. Such an approach would be prohibitively time consuming. Therefore, the algorithm makes use of the following two approximate functions: One which takes coordinates for the LR directly to the SOM projection and associated elevation, and a second which takes coordinates from SOM and computes directly the corresponding position in the input files. Both functions are linear, requiring less computation. In addition sufficient accuracy is preserved (i.e., better than 15 m) by evaluating the pair of functions for regions no larger than 25 km square. There is a different pair of functions used for each of these regions making up the swath. Applying such a method instead of exact coordinate transformations has significantly decreased MISRSIM processing (i.e., 4-5 times) without degradation of the needed accuracy.

#### MISRSIM Rendering Algorithm

The following is a high level description of the MISRSIM rendering algorithm. Certain of these operations involve methods of optimization described in detail in the next section.

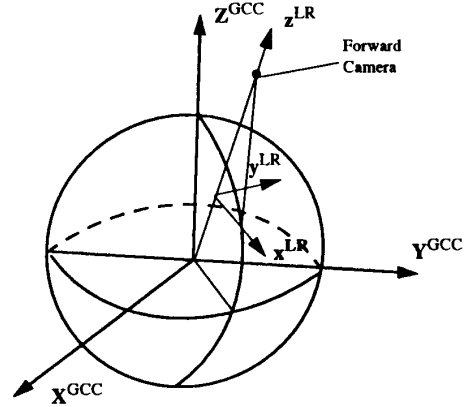


Figure 1: Relation between the GCC and LR system

For a given camera, the following steps are performed:

- For each orbit position, loop over the following steps:
  - Calculate position of camera in GCC.
  - Calculate position of swath center in GCC.
  - Construct matrices for transformation from camera position to surface intercept in LR.
- For each pixel (or subpixel) in a camera, loop over the following steps:
  - Construct ray vectors for each camera pixel (and subpixel) in LR.
  - Obtain initial range along ray.
  - Step along ray until the DEM is intersected.
  - Calculate ground spread of the intersection point.
  - Retrieve the output radiance for the pixel (or subpixel).
- End loop.
- If subpixeling is used, sum the radiances corresponding to an output camera pixel.
- Save the range of the intersection to use for the initial range estimate of the next line.
- End loop.

#### MISRSIM RENDERING OPTIMIZATIONS

##### Initial Range Calculation

Ray casting is a simple algorithm which can be optimized only in a few ways. Either the time required to step along a ray must be reduced, or the number of steps needed to intersect the surface must be reduced. The latter can be exploited by selecting a good starting point. The idea for doing this is shown in Figure 2. As shown, the ray A is parallel to ray B. This means that B will go at least as "far" as A. In other words, the distance from the intersection of B with the surface to the current orbit position, projected to the LR xy-plane, is at least the projected distance from the intersection of A to the current orbit position. That is,  $\|I_B - O_B\|_{xy} \geq \|I_A - O_B\|_{xy}$ . The starting point  $S_B$  is chosen such that  $\|S_B - O_B\|_{xy} = \|I_A - O_B\|_{xy}$ .

In reality, there is not a ray at the previous orbit position that is exactly parallel to the current ray. But there are some rays that are close to parallel. The following was used for pixel  $p$ , orbit position  $n$ , to calculate  $\|S_{p,n} - O_n\|_{xy}$ :

$$\min (\|I_{p,n-1} - O_n\|_{xy}, \|I_{p+1,n-1} - O_n\|_{xy}, \|I_{p-1,n} - O_B\|_{xy})$$

This works well in practice; a typical ray needs only one or two steps past the starting point to intersect the surface.

Note that this initial range calculation requires that the pixel ray intersections to be calculated in a particular order. For aft looking cameras, this requires the orbit to be incremented backwards (i.e.,

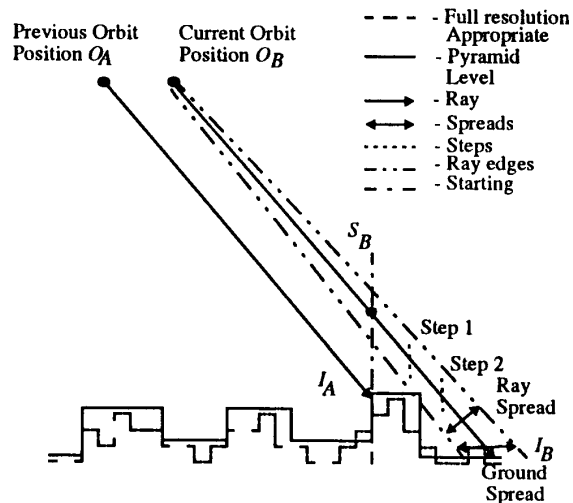


Figure 2: Ray casting

starting with the last orbit position). In addition, pixels 1 and 1504, as well as the entire first line of pixels, cannot use this initial guess, because the intersection of surrounding pixels is not available. Instead, the initial range is determined by finding the intersection of the ray with a plane at the maximum elevation (determined previously for the particular DEM used).

#### Image Pyramids

An image pyramid is built as follows: Starting with an image described by  $I_1$  with  $m \times n$  pixels, a coarser description of the image,  $I_2$ , with  $m/2 \times n/2$  pixels is made. This can be performed in a number of ways: e.g., straight averaging or convolution with a Gaussian and then resampling. Additional images ( $I_3$ ,  $I_4$ , etc.) are built in the same way. The set  $(I_1, I_2, \dots, I_n)$  is referred to as a  $n$  level image pyramid.  $I_1$  is referred to as level 1 of the pyramid,  $I_2$  as level 2, etc.

Image pyramids are made use of in MISRSIM in two ways. In the algorithm described above, the output radiance is found by averaging over pixels, but instead of doing this explicitly, an image pyramid which contains this averaging can be used. To average over a spread  $S$ , the radiance value at the pyramid level where the pixel size is  $S$  is used. Generally, there will be no pyramid level with a pixel size exactly  $S$ . Therefore, interpolation is performed between the two closest levels. The second way that image pyramids are utilized is in speeding up the calculation of the intersection of a ray with the DEM by reducing the number of steps. If the spread of a ray on the ground is 250 meters, then the output is not sensitive to features that are 10 meters in size. There is no reason that the intersection calculation needs to be more accurate than the order of the spread. A coarser DEM is then made use of when performing the intersection calculation. Because the coarser DEM has fewer pixels, the computation is reduced.

Note that the spread of a ray on the ground is not known until after the intersection is found, at which point, it is too late to use in the intersection calculation. However, a lower bound is the spread of a ray for a surface normal to the direction of the ray (see Figure 2). This spread, called the ray spread (as opposed to the ground spread), is what is used in the intersection calculation.

#### DATA VALIDATION

Two methods have been used to validate the simulated data. First, images covering the same area from pairs of viewing angles

were examined in a stereo viewer. Visually the topography was found to be registered with the features in the images. Second, features were identified in the simulated images, and the image coordinates of those features for all nine camera were measured. Those image coordinates provided the means to define the exterior orientation of the cameras by accessing the navigation data from the orbit program. Then, the ground coordinates of the particular feature were computed via Least-Squares adjustment with a mathematical model based on the photogrammetric collinearity condition. The differences between computed ground coordinates and the ground coordinates from the original input were examined. The resultant RMS errors (82 m horizontal) were expected due to the accuracy of the manual monoscopic measurement of the image coordinates. The conclusion is that there are no significant errors introduced by the algorithm.

#### FUTURE EXPERIMENTS

This paper describes the work which has been completed by the time of publication. At the IGARSS, the authors will present the results of additional experiments and improvements to the MISRSIM program. This future work is outlined below:

##### Orbit Perturbations

The current orbit program will be modified to model the possible magnitude and frequency of perturbations to spacecraft position and pointing. Simulated imagery will be generated with these perturbations, and then image matching will be performed between images covering the same area. From this, the frequency of match points required to register these images can be estimated.

##### Atmospheric Refraction

The current version of the code does not account for the effects of atmospheric refraction. It has been determined that for the resolution of the MISR imagery the atmospheric refraction can be accounted for by applying a constant offset to the resultant images. This offset will be different for each of the nine viewing angles.

##### Contrast Reduction

The code will be modified to simulate the radiometric differences between images from different viewing angles. The effects of these differences on the ability to do image matching will be examined. Initially, a simple contrast reduction filter will be applied to the data. At a later date, a bi-directional reflectance distribution function (BRDF) model will be implemented, which will account for effects of reflectance anisotropy at the different viewing angles.

#### ACKNOWLEDGMENTS

The work described in this paper was carried out at the Jet Propulsion Laboratory, California Institute of Technology, under contract with the National Aeronautics and Space Administration.

The authors would like to thank Daniel Stanfill for supplying the initial RENDERER code and Steven Adams for supplying Landsat imagery and registered DEMs. Both are part of the Digital Image Animation Laboratory at JPL.

#### REFERENCES

- [1] Diner, D.J., C.J. Brugge, T. Deslis, V.G. Ford, L.E. Hovland, D.J. Preston, M.J. Shterenberg, E.B. Villegas, and M.L. White. "Development status of the EOS Multi-angle Image SpectroRadiometer (MISR)." *SPIE Proc.* 1939 (1993): 94-103.
- [2] Stanfill, D.F. "Using Image Pyramids for the Visualization of Large Terrain Data Sets." *International Journal of Imaging Systems and Technology*, Vol. 3 (1991): 157-166.